Evidence for chaos in an experimental time series from serrated plastic flow

S. Venkadesan,[1] M. C. Valsakumar,[2] K. P. N. Murthy,[2] and S. Rajasekar[3]
[1]*Materials Technology Section, Materials Development Division, Indira Gandhi Center for Atomic Research, Kalpakkam 63 102, Tamil Nadu, India*
[2]*Theoretical Studies Section, Materials Science Division, Indira Gandhi Center for Atomic Research, Kalpakkam 603 102, Tamil Nadu, India*
[3]*Department of Physics, Manonmaniam Sundaranar University, Tirunelveli 627 002, Tamil Nadu, India*

An experimental time series from a tensile test of an Al-Mg alloy in the serrated plastic flow domain is analyzed for signature of chaos. We employ state space reconstruction by embedding of time delay vectors. The minimum embedding dimension is found to be 4 and the largest Lyapunov exponent is positive, thereby providing *prima facie* evidence for chaos in an experimental time series of serrated plastic flow data. [S1063-651X(96)04206-7]

PACS number(s): 62.20.Fe, 83.50.Ws, 83.50.By

I. INTRODUCTION

Instabilities in plastic deformation of metals and alloys often manifest themselves as serrated yield drops in tensile tests. These yield drops have been attributed to the phenomenon of dynamic strain aging which results from the interaction of mobile dislocations and the solute atoms. There have been several studies, experimental [1–6] and theoretical [7–20], to understand the different aspects of this serrated flow phenomenon. We shall desist from embarking on a survey of the rich and growing literature on this fascinating subject and only refer to some recent reviews [21–28]. Instead, in this paper we shall focus attention on a very specific issue—Is there a low dimensional chaotic dynamics underlying and responsible for the irregular oscillations in the load signals observed as a function of time, during tensile tests under constant displacement rate control? We present a dynamical analysis of time series of serrated plastic flow obtained from an experiment. We describe in Sec. II a tensile test carried out by one of us (S.V.) on a specimen of Al-Mg alloy. In Sec. III we present a numerical analysis of the experimental time series. Our analysis is based on state space reconstruction by the embedding of time delay vectors. We have employed some of the recent developments in this field to obtain the state space dimension, delay time, and the largest Lyapunov exponent. The state space dimension is found to be 4. This is indicative of the minimum number of macroscopic variables essential for modeling the dynamics underlying unstable plastic flow. Also, we find that the Lyapunov exponent is positive. Section IV summarizes briefly the principal conclusions of our study.

II. SERRATED YIELD EXPERIMENTS

The material used in the investigation is an alloy of aluminum with 3 wt% magnesium, obtained as 1 mm thick sheets. Tensile test samples with a gauge length of 25 mm were punched out from the sheets. The specimens were annealed in air at 693 K for 120 min, followed by quenching in water. The samples were stored at 263 K, till the start of the test. Tensile tests were carried out on an Instron 1126 tensile testing machine, fitted with a 5 kN load cell. The tests were carried out in the monotonic and constant specimen displacement rate (SDR) mode, which could be chosen in the range 0.000 1 mm/s to a maximum of 3 mm/s. A constant temperature bath which enables test temperatures in the range 263–373 K with a control accuracy of ± 0.1 K was used. The load signal obtained as a function of time was recorded and stored digitally using a high speed data acquisition system. The data acquisition system consisted of an IBM PC/AT compatible computer, a Metrabyte Iso-4 multiplexer, Metrabyte Das-8 analog-to-digital converter board running under LABTECH Notebook software. The data acquisition rate was optimized for each test depending on the SDR value. A few blank runs established that the noise level was below 2.5 mV. The zero level signal was preset to a negative value to ensure that all the data acquisition occurred in the linear domain of the signal processing instrument, while ensuring maximum output signal levels. Figure 1 depicts the complete load (more exactly the voltage proportional to the load) as a function of time (or strain), corresponding to a test at 310 K and at an SDR of 0.008 mm/s. Purely elastic response of the system for small strain and the imminent fracture due to triaxiality induced by necking for large strain are clearly seen. The load oscillations characteristic of a dynamically strain aging material is evident within the window indicated in Fig. 1. The width of the window being finite, the total amount of data collected gets restricted in these tensile tests. This inherent limitation in the total number of data points that can be generated is going to constrain the scope of time series analysis of all such experiments.

For all the subsequent analysis we use the data corresponding to the serrated flow shown in the window. We observe that there is a monotonic rise in the signal with time. This is due to work hardening, the basis of which is well understood, see for example [29]. Briefly stated, on an average, the obstacles to dislocation mobility becomes stronger and more in number as the strain increases, making the ma-

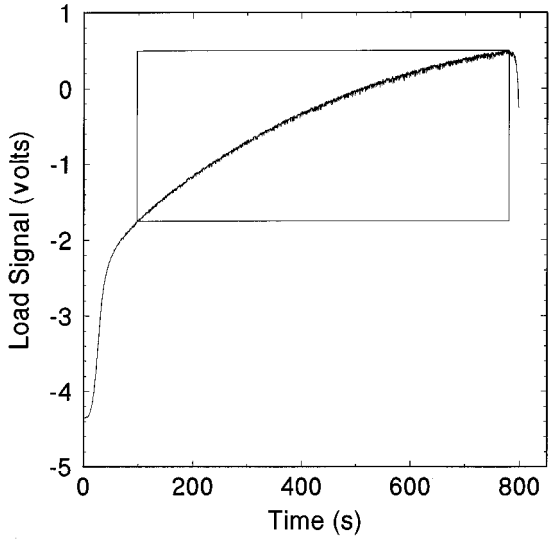

FIG. 1. Load signal versus time in a tensile test on the Al-Mg alloy. The box indicates the serrated plastic flow region used for the time series analysis.

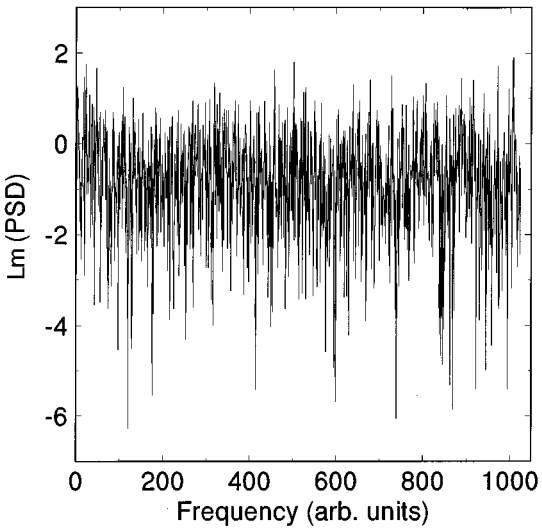

FIG. 3. Logarithm of the power spectral density (PSD) of the serrations shown in Fig. 2.

terial harder. In our analysis we eliminate the drift component due to work hardening by fitting the data to a second order polynomial and subtracting it from our data set. As can be seen from Fig. 2, the fluctuations due to serrated yield are left intact in the resultant stationary time series.

III. ANALYSIS OF EXPERIMENTAL TIME SERIES

The analysis of the experimental time series, depicted in Fig. 2 is described in this section. As a first step, we calculate the power spectrum, which would tell us whether the time series represents a periodic or a nonperiodic state. For a periodic state the power spectrum would contain sharp fundamental frequency components and their harmonics. A nonperiodic state, however, would lead to a broadened spectrum. The power spectrum of the experimental time series is depicted in Fig. 3; it is broad, like that of noise. The next task is to distinguish whether the broad power spectrum is of stochastic or deterministic (chaotic) origin. Making such a distinction is possible because chaos admits *short time* predictability and defies only *long time* forecasting. The long time unpredictability is a direct consequence of the dynamics being *extremely sensitive to initial conditions*—a hallmark of all chaotic systems. On the other hand there is no predictability, short time or otherwise for stochastic systems. The parameter that captures the time scale beyond which the chaotic dynamics loses predictability is the Lyapunov exponent λ. Simply stated, the Lyapunov exponent characterizes the time evolution of the distance between two dynamical trajectories, starting from neighboring points in the phase space. For a dynamics occurring in an m-dimensional phase space, we can define, in fact, a spectrum of m Lyapunov exponents, characterizing the evolution of distance between two dynamical trajectories along m orthoganal directions. For a dynamics to be chaotic, there must exist at least one positive Lyapunov exponent. Therefore to distinguish chaos from noise it is sufficient if we estimate the value of the largest Lyapunov exponent and see if it is positive, and to this task we turn our attention below.

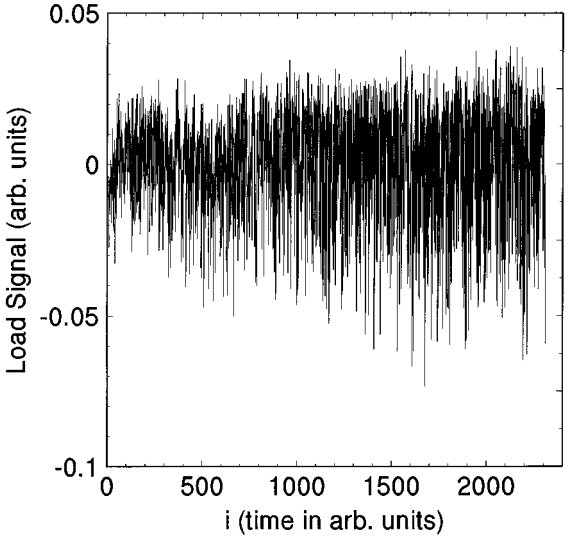

FIG. 2. Serrated yield time series after elimination of drift.

Let $\{x_j \equiv x(j\Delta t): j=1,N\}$ denote the time series, depicted in Fig. 2, consisting of a load measured at regular intervals. For the time series under analysis $N=2310$, and, $\Delta t=0.303$ s. The first step towards the calculation of the largest Lyapunov exponent is the construction of the state space by the embedding of time delay vectors. This technique was first discovered by Ruelle in the early eighties and is described in [30]. There have since been numerous developments, see for example, the recent reviews [31–35]. The method essentially consists of constructing m dimensional, L-delay vectors, defined by $\{\vec{X}_i = (x_i, x_{i+L}, x_{i+2L}, \ldots x_{i+(m-1)L})\}$. The time ordered sequence of vectors, $\{\vec{X}_i : i=1,2, \ldots N-(m-1)L\}$, defines a trajectory in the m-dimensional phase space, induced by a dynamics

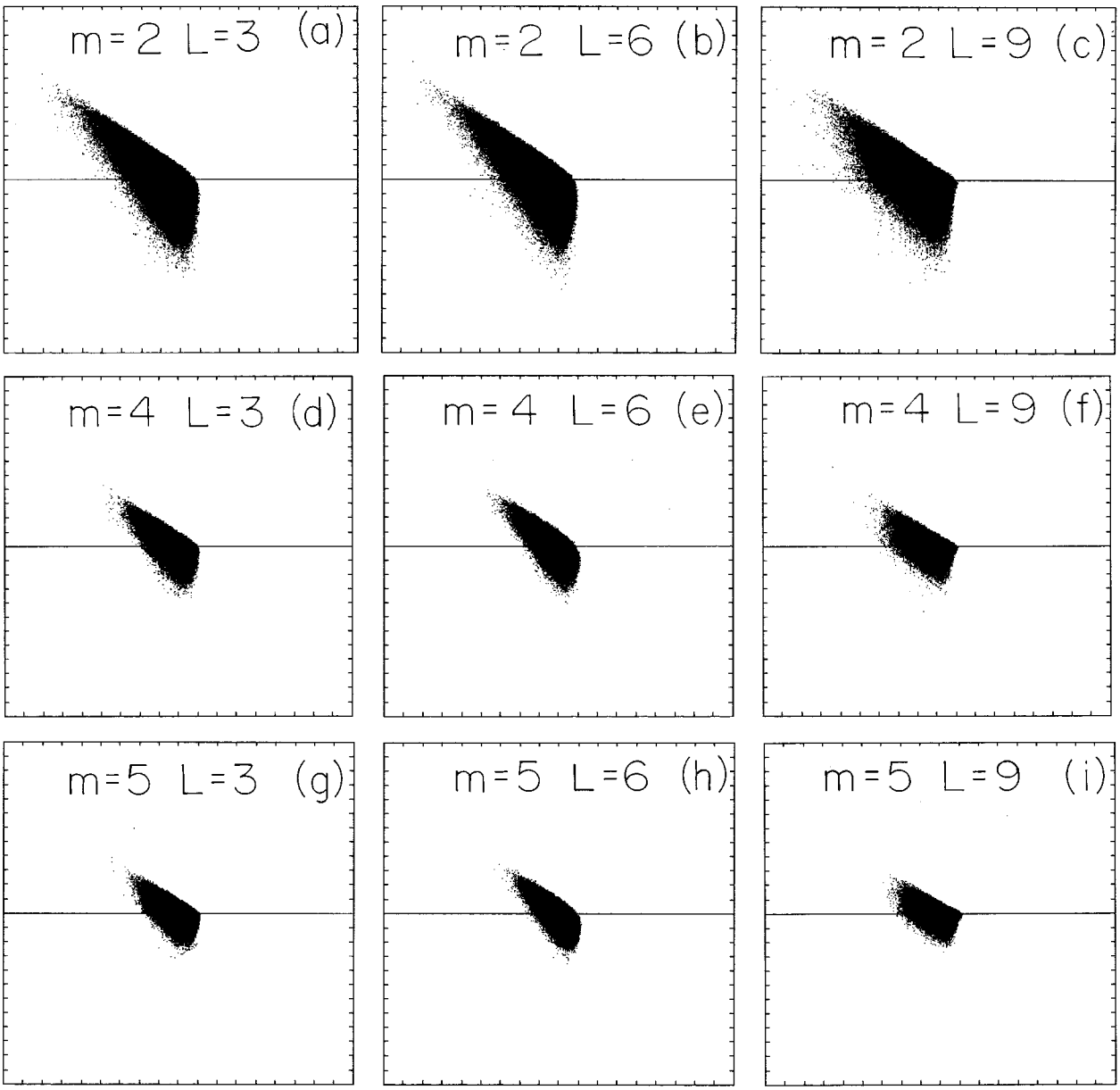

FIG. 4. Local exponential divergence plots for typical values of m and L. The abscissa is $\ln[d_{i,j}(0)]$ and the ordinate is $\ln[d_{i,j}(k)]/\ln[d_{i,j}(0)]$, see text. Also, all the figures have the same scale.

$\vec{X}_{i+1}=F(\vec{X}_i)\equiv F^i(\vec{X}_1)$. The dynamics F retains the characteristics (like the Lyapunov exponent) of the actual but unknown dynamics, if the embedding dimension m and less importantly the delay time L, are chosen *properly*. This equivalence of F to the unknown dynamics is assured by embedding theorems [36]. The question arises then as to the criterion we must adopt to ensure a *proper* choice of m and L. Intuitively, two vectors which are actually very far apart, may look close to each other when represented in a lower dimension. Thus in the passage from a dimension m to $(m+1)$, one can detect false neighbors from true ones. When m is greater than or equal to the *correct* embedding dimension, say m_o, the number of false neighbors would be zero. Based on this notion, several methods have been developed [37–39] and we employ in this paper a recent technique proposed by Gao and Zheng [40] that implements this idea dynamically. Let $d_{i,j}(0)=\|\vec{X}_i-\vec{X}_j\|$ be the Euclidean distance between the vectors $\vec{X}_i$ and $\vec{X}_j$. This distance gets mapped to $d_{i,j}(k)=\|\vec{X}_{i+k}-\vec{X}_{j+k}\|$ by k iterations of the dynamics F. We calculate $\ln[d_{ij}(k)/d_{ij}(0)]$ and plot it against $\ln[d_{ij}(0)]$ for all possible pairs of vectors. This constitutes the local exponential divergence plot for a given value of m and L, with k being fixed at a chosen value. If m is much smaller than m_o, the large number of false neighbors would generate excessively large positive values in the local exponential divergence plot. When m is increased, the exponential divergence plots would become more and more compact. When m increases from m_o to m_o+1, there would not be any significant or easily discernible change in the local exponential divergence plot. The same observations hold good for L also. More quantitatively we define $\gamma\equiv\langle\ln[d_{ij}(k)/d_{ij}(0)]\rangle$ where the angular brackets denote an average over all possible pairs

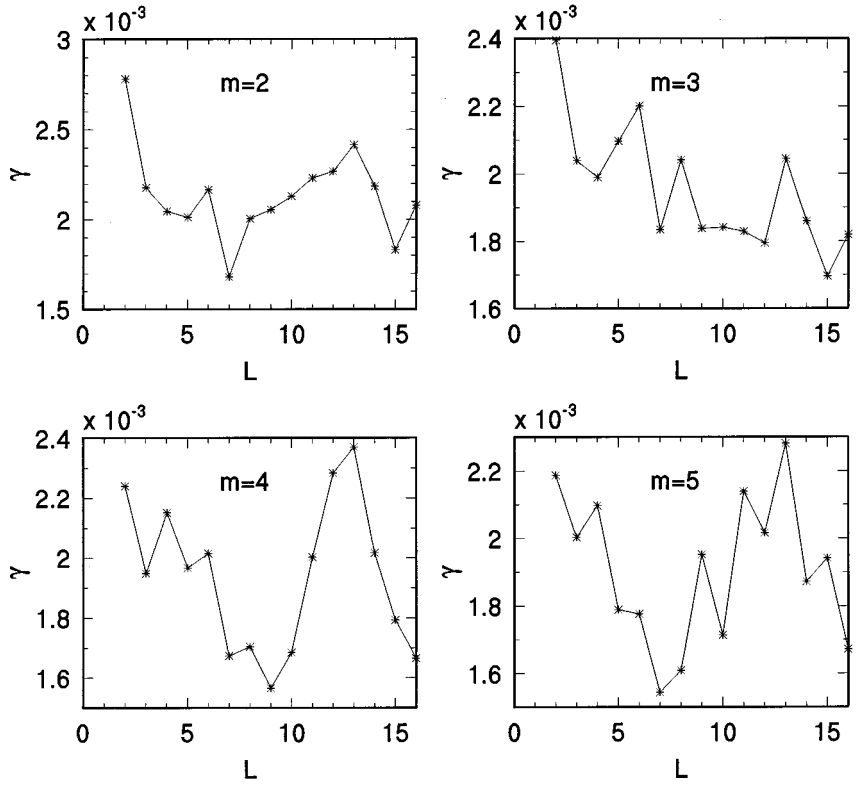

FIG. 5. γ versus L for typical values of m and L. Note γ shows a minimum at $m=4$ and $L=9$.

of vectors. As m increases, γ will decrease and beyond $m=m_o$, the decrease will not be significant. For the selected $m=m_o$, the quantities γ plotted against L, would exhibit minima at say $L=L_o$, which defines the optimal delay time.

Figure 4 depicts a set of local exponential divergence plots, for representative values of m and L. The value of $m=4$ yields a compact plot, for $L=9$. Figure 5 depicts γ versus L, for various values of m. We find $m=4$ is the minimal acceptable dimension. We also see from Fig. 5 that γ exhibits a minimum at $L=9$ for $m=4$. Thus we take $m\equiv m_o=4$ as the acceptable minimum embedding dimension and $L=L_E=9$, as the proper choice of delay time. Then we proceed to calculate γ as a function of k. To reduce the effect of tangential flow, we consider only those vectors $\vec{X}_i$ and $\vec{X}_j$ with $|j-i|>\omega$, where we take $\omega=(m-1)L$ as recommended by Gao and Zhang [40]. In Fig. 6, we depict γ as a function of k for the case when $m=4$ and $L=9$ and for k from 1 to 200, with $d_{ij}(0)\leqslant 750$, measured in units of the minimum distance between two delay vectors. A linear least square fit for $\gamma(k)$ versus k yields a positive slope, $S=2.5\times10^{-4}$ and nearly zero intercept. The average value of the largest Lyapunov exponent, λ is given by $\lambda=S/[\Delta t\ln(2)]=1.1\times10^{-3}$ *bits per second*. The linear increase of γ with k, the zero intercept and the positivity of the Lyapunov exponent, indicate that there is indeed a *prima facie* evidence for a four dimensional chaotic dynamics as being responsible for the instabilities in the plastic flow as manifest in the serrated yielding phenomenon.

It is indeed desirable to demonstrate the constancy of the Lyapunov exponent as $d_{ij}(0)$ is decreased to smaller and smaller values. We are not able to demonstrate this and the reasons for this are as follows. The data set we have is small; when $d_{ij}(0)$ is taken as small, the number of delay vectors that become available for estimating γ is small and consequently the statistical fluctuations (errors) are large. Instead, we calculate γ versus k for $d_{ij}(0)\leqslant\alpha$, where $\alpha=750$, 650, 600, and 550. α is expressed in units of the resolution of the attractor, in other words, in units of the minimum Euclidian distance between two delay vectors constructed from the time series. These are shown in Fig. 7. The curves are linear and coincide for k up to 120 or so. It is true that a stochastic process, represented in a finite precision, might lead to exponential divergence of neighboring phase

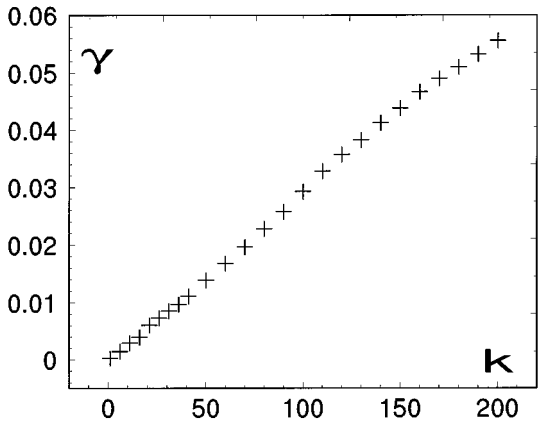

FIG. 6. γ versus k (time) for the experimental time series at $m=4$ and $L=9$, for $d_{ij}(0)\leqslant750$.

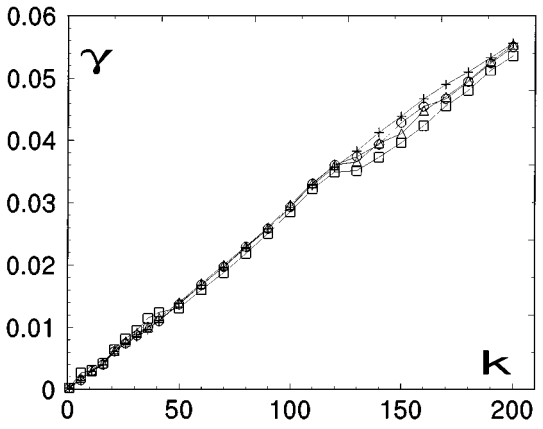

FIG. 7. γ versus k time series at $m=4$ and $L=9$, for $\alpha=750(+)$, $650(\bigcirc)$, $600(\triangle)$, and $550(\square)$.

space trajectories. The probability for this to occur increases as $d_{ij}(0)$ is decreased. However, for a stochastic process one would not get any systematic variation of γ with k, as we show below.

We construct a time series from Gaussian white noise with the same mean and variance as that of the experimental time series. Figure 8 depicts γ versus k for $\alpha=750$, and 550, that correspond to the two extreme values considered for the experimental time series. The embedding dimension is four and the delay time is nine, and these are the same ones used for analysis of the experimental time series. The negative value of γ for $\alpha=750$ is due to the fact that all possible delay vectors have been used for the analysis. However for $\alpha=550$ we find that γ is positive for values of k up to 120. The important point is that γ does not bear any systematic, linear or otherwise, relation to k, in contrast to what we observe for the experimental time series. Thus we can reasonably conclude that the experimental time series is not stochastic.

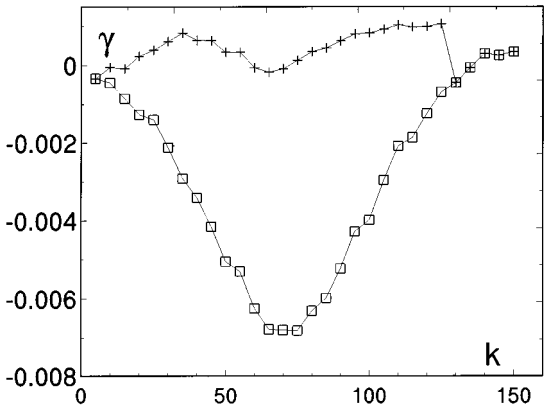

FIG. 8. γ versus k for the Gaussian white noise with the same mean and variance as that of the experimental time series, with $m=4$, $L=9$, for $\alpha=750(\square)$, and $550(+)$.

IV. CONCLUSIONS

In this paper we have reported a detailed numerical analysis of an experimental serrated flow time series. We have employed state space reconstruction by an embedding of time delay vectors. We find that the minimal embedding dimension is 4 and optimal delay time is nine units. The largest Lyapounov exponent is found positive, indicative of chaos. Thus we have shown that there is a *prima facie* reason to expect a low dimensional chaotic dynamics underlying the serrated flow phenomenon. The immediate task is to investigate the nature of the strange (chaotic) attractor. The experimental data we have at present is infrequent (Δt is large) and inadequate (N is small), for such an analysis. A dedicated experiment on serrated yield phenomenon tuned specially for dynamical analysis is underway.

ACKNOWLEDGMENTS

The experimental work was carried out by one of us (S.V.) at the University of Western Australia, Perth.

[1] E. Pink and A. Grinberg, Mater. Sci. Eng. **51**, 1 (1981).
[2] S. L. Mannan, K. G. Samuel, and P. Rodriguez, Trans. Ind. Inst. Metals **36**, 313 (1983).
[3] G. G. Saha, P. G. McCormick, and P. Rama Rao, Mater. Sci. Eng. **62**, 187 (1984).
[4] S. Venkadesan, C. Phaniraj, P. V. Sivaprasad, and P. Rodriguez, Acta Metall. Mater. **40**, 569 (1992).
[5] S. Venkadesan, P. Rodriguez, K. A. Padmanabhan, P. V. Sivaprasad, and C. Phaniraj, Mater. Sci. Eng. **154**, 69 (1992).
[6] S. Venkadesan, S. Venugopal, P. V. Sivaprasad, and P. Rodriguez, Mater. Trans. Jpn. Inst. Metals **33**, 1040 (1992).
[7] A. H. Cottrell, Philos. Mag. **44**, 829 (1953).
[8] S. R. Bodner and A. Rosen, J. Mech. Phys. Solids **15**, 63 (1967).
[9] P. Penning, Acta Metall. **20**, 1169 (1972).
[10] P. G. McCormick, Acta Metall. **20**, 351 (1972).
[11] A. Van den Beukel, Phys. Stat. Sol. (a) **30**, 197 (1975).
[12] A. Van den Beukel, Acta Metall. **28**, 965 (1980).
[13] G. Ananthakrishna and D. Sahoo, J. Phys. D **14**, 2081 (1981).
[14] G. Ananthakrishna and D. Sahoo, J. Phys. D **14**, 2091 (1981).
[15] G. Ananthakrishna and M. C. Valsakumar, J. Phys. D **15**, l171 (1982).
[16] M. C. Valsakumar and G. Ananthakrishna, J. Phys. D **16**, 1055 (1983).
[17] G. Ananthakrishna and M. C. Valsakumar, Phys. Lett. A **95**, 69 (1983).
[18] L. P. Kubin, Y. Estrin, and Ph. Spiesser, Res. Mechanica **10**, 25 (1984).
[19] P. Hahner, Mater. Sci. Eng. A **164**, 23 (1993).
[20] L. Schlipf, Scr. Metall. Mater. **31**, 909 (1994).
[21] E. O. Hall, *Yield Point Phenomena in Metals and Alloys* (McMillan, London, 1970).
[22] J. D. Baird, Metall. Rev. **16**, 1 (1971).
[23] R. E. Reed-Hill and Tuling Zhu, High Temp. Mater. Process **6**, 93 (1984).
[24] P. Rodriguez, Bull. Mater. Sci. **6**, 653 (1984).

[25] P. Rodriguez, in *Encyclopaedia of Materials Science and Engineering*, edited by R. W. Cahn, Supplementary Vol. 1 (Pergamon, Oxford, 1988), p. 504.
[26] P. G. McCormick, Acta Metall. **36**, 3061 (1988).
[27] Y. Estrin and P. G. McCormick, Acta Metall. Mater. **39**, 2977 (1991).
[28] Y. Estrin, L. P. Kubin, and E. C. Aifantis, Scr. Metall. Mater. **29**, 1147 (1993); see also papers in the View Point Set No. 21 **29**, 1148 (1993).
[29] *Contitutive Equations in Plasticity*, edited by A. S. Argon (MIT, Cambridge, MA, 1975).
[30] N. H. Packard, J. A. Crutchfield, J. D. Farmer, and R.S. Shaw, Phys. Rev. Lett. **45**, 712 (1980).
[31] D. Farmer, E. Ott, and A. Yorke, Physica D **7**, 153 (1980).
[32] J. P. Eckmann and D. Ruelle, Rev. Mod. Phys. **57**, 617 (1985).
[33] J. D. Farmer and J. J. Sidorowich, Phys. Rev. Lett. **59**, 845 (1987).
[34] M. Casdagh, S. Eubank, J. D. Farmer, and J. Gibson, Physica D **51**, 52 (1991).
[35] H. D. I. Aberbanel, Rev. Mod. Phys. **65**, 1331 (1993).
[36] F. Takens, in *Dynamical Systems and Turbulence*, Vol. 898 of Lecture Notes in Mathematics, edited by D. A. Rand and L. S. Young (Springer-Verlag, Berlin, 1981) p. 366.
[37] A. Cenys and K. Pyragus, Phys. Lett. A **129**, 227 (1988).
[38] Z. Aleksic, Physica D **52**, 362 (1991).
[39] W. Liebert, K. Pawelzik, and H. G. Schuster, Europhys. Lett. **14**, 521 (1991).
[40] J. Gao and Z. Zheng, Phys. Rev. E **49**, 3807 (1994).